

Dandelion-like Co_3O_4 mesoporous nanostructures supported by Cu foam for efficient oxygen evolution and lithium storage

Fang Wang,^{‡c} Zhi-Bo Liu,^{‡d} Ke-Xin Wang,^{‡c} Xiao-Dong Zhu,^{*a,b} Xiu-Hua Fan,^c Jian Gao,^c Yu-Jie Feng,^b Ke-Ning Sun^b and Yi-Tao Liu^{*d}

^aState Key Laboratory of Urban Water Resource and Environment, Harbin Institute of Technology, Harbin 150090, China

^bAcademy of Fundamental and Interdisciplinary Sciences, Harbin Institute of Technology, Harbin 150080, China

^cDepartment of Chemistry, Harbin Institute of Technology, Harbin 150001, China.

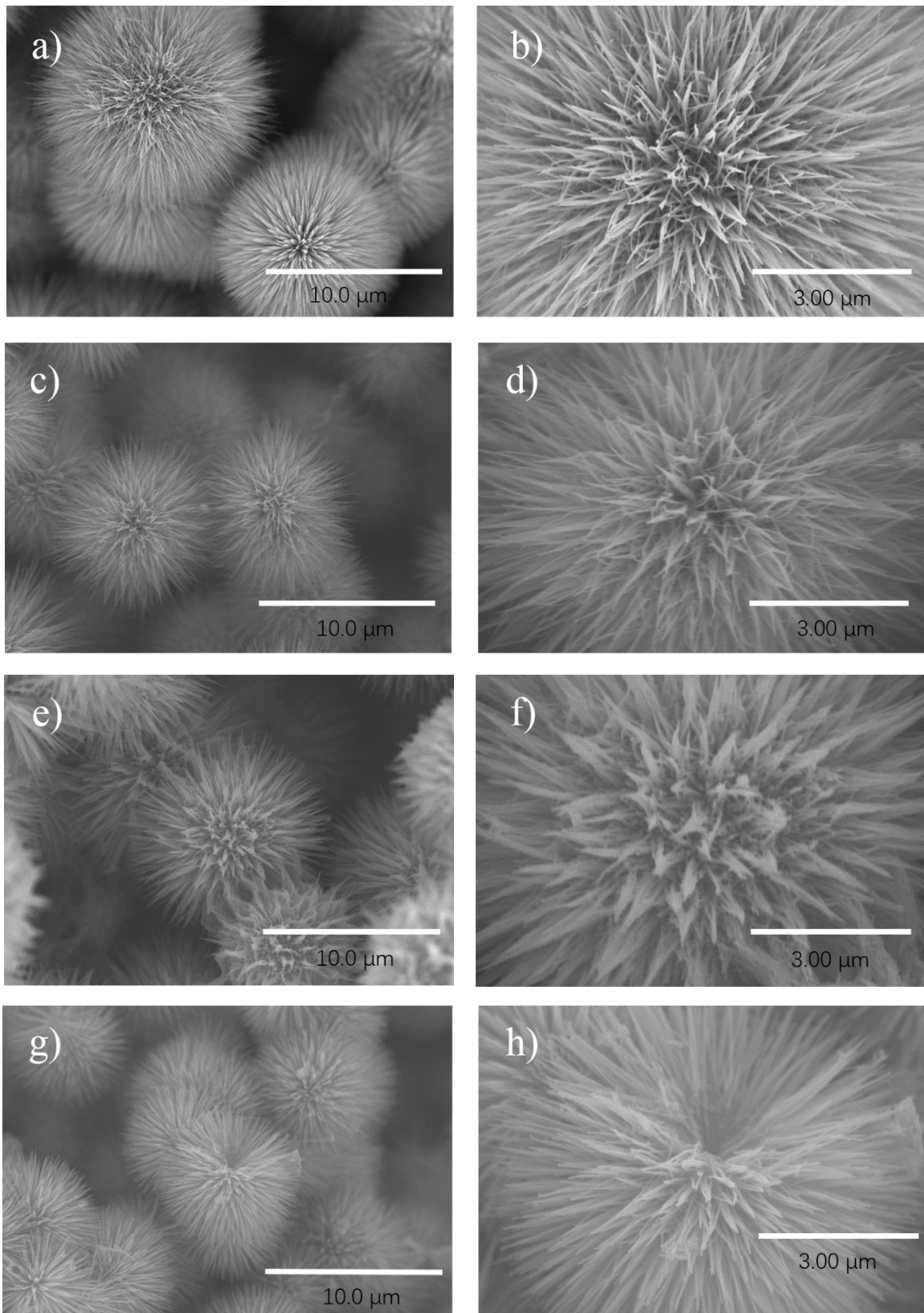
^dState Key Laboratory of Organic–Inorganic Composites, Beijing Key Laboratory of Electrochemical Process and Technology for Materials, Beijing University of Chemical Technology, Beijing 100029, China.

Experimental Section

Preparation of $\text{Co}_3\text{O}_4@\text{Cu}$ foam: The $\text{Co}_3\text{O}_4@\text{Cu}$ foam was prepared by a combination of hydrothermal synthesis and annealing. Briefly, $\text{Co}(\text{NO}_3)_2 \cdot 6\text{H}_2\text{O}$ (1 mmol), NH_4F (2.7 mmol) and $\text{CO}(\text{NH}_2)_2$ (7.5 mmol) were dissolved in deionized water (30 ml) and stirred for 30 min. Then, the fully mixed solution and Cu foam ($\varphi = 12$ mm) were transferred to a Teflon-lined stainless steel autoclave (50 ml), and heated at 110 °C for 12 h. After the autoclave was cooled naturally to ambient temperature, the precipitate was washed by absolute alcohol and deionized water, and vacuum-dried at 60 °C overnight. Finally, the precipitate was annealed at different temperatures (200, 300, 400 and 500 °C) for different times (1, 2, 3 and 4 h). For comparison, the Co_3O_4 powder was prepared by annealing at 300 °C for 2 h in the absence of Cu foam.

Electrochemical testing: The OER properties were measured in 1M KOH aqueous solution by using a three-electrode mode on an electrochemical workstation (CHI 660D, CH Instruments). The Pt net and SCE were used as counter and reference electrodes, respectively. All potentials were converted to the reversible hydrogen electrode (RHE) based on the equation $E(\text{vs. RHE}) = E(\text{vs. SCE}) + 0.244 + 0.059 \times \text{PH}$. The OER activities were investigated by linear sweep voltammetry (LSV) at a scan rate of 5 mV s⁻¹ and the LSV data were made with an 80% ohmic drop (iR) correction tested by impedance spectroscopy. Electrochemical impedance spectroscopy (EIS) was performed by applying an AC voltage of 5 mV from 100 kHz to 0.01 Hz. CR-2025 coin-type cells were assembled to evaluate the lithium storage performance of the $\text{Co}_3\text{O}_4@\text{Cu}$ foam inside an argon-filled glove box. The microporous polypropylene membrane, lithium foil, and 1 M solution of LiPF_6 in ethylene carbonate and dimethyl carbonate (volume ratio = 1:1) were used as the separator, counter and reference electrode, and electrolyte, respectively. The assembled cells were allowed to soak overnight, and the electrochemical tests were performed on a LAND battery testing unit. Cyclic voltammetry (CV) was performed using a CHI 660E electrochemical workstation between 0.01–3.00 V (vs. Li^+/Li) at a scan rate of 0.1 mV s⁻¹. Electrochemical impedance spectroscopy (EIS) was performed by applying an AC voltage of 5 mV from 100 kHz to 0.01 Hz.

Supplementary Figures and Tables



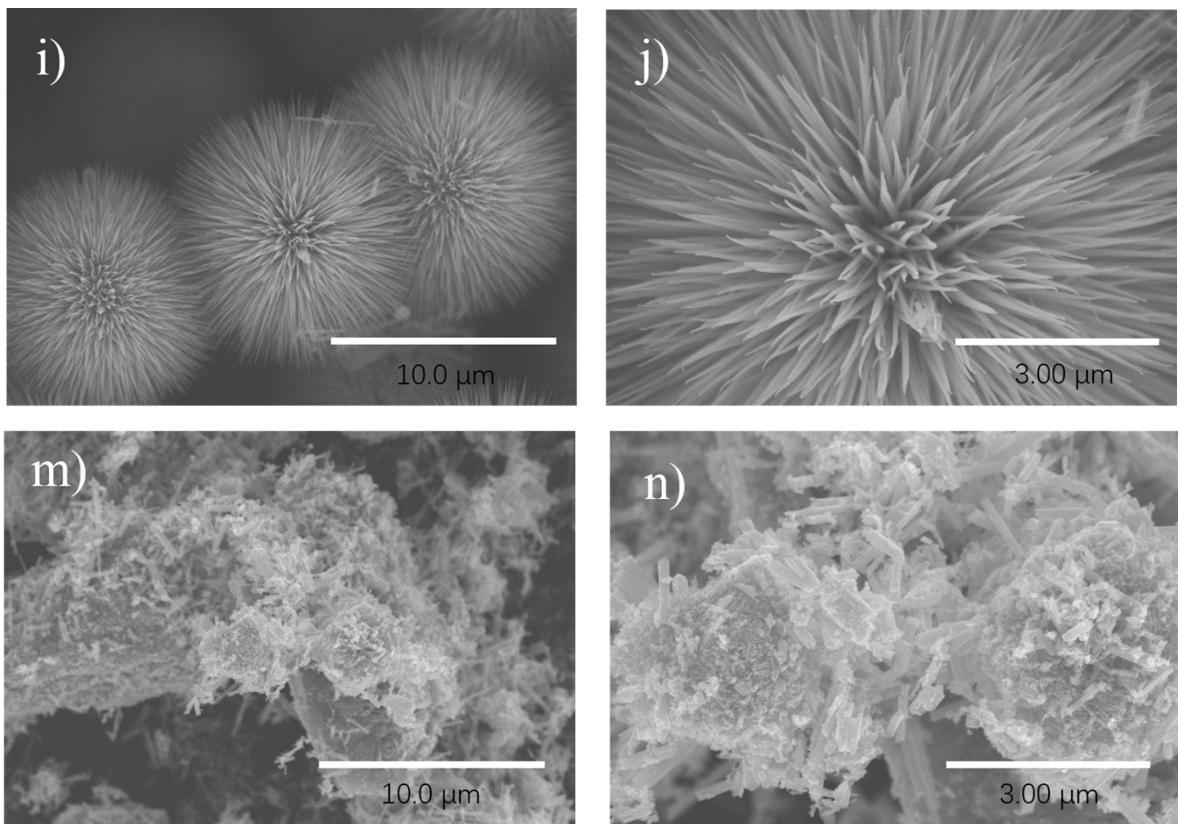


Fig. S1 – Low- and high-magnification SEM images of (a, b) $\text{Co}_3\text{O}_4@\text{Cu}$ foam-300°C-2h, (c, d) $\text{Co}_3\text{O}_4@\text{Cu}$ foam-400°C-2h, (e, f) $\text{Co}_3\text{O}_4@\text{Cu}$ foam-500°C-2h, (g, h) $\text{Co}_3\text{O}_4@\text{Cu}$ foam-300°C-1h, (i, j) $\text{Co}_3\text{O}_4@\text{Cu}$ foam-300°C-4h, and (m, n) Co_3O_4 powder-300°C-2h.

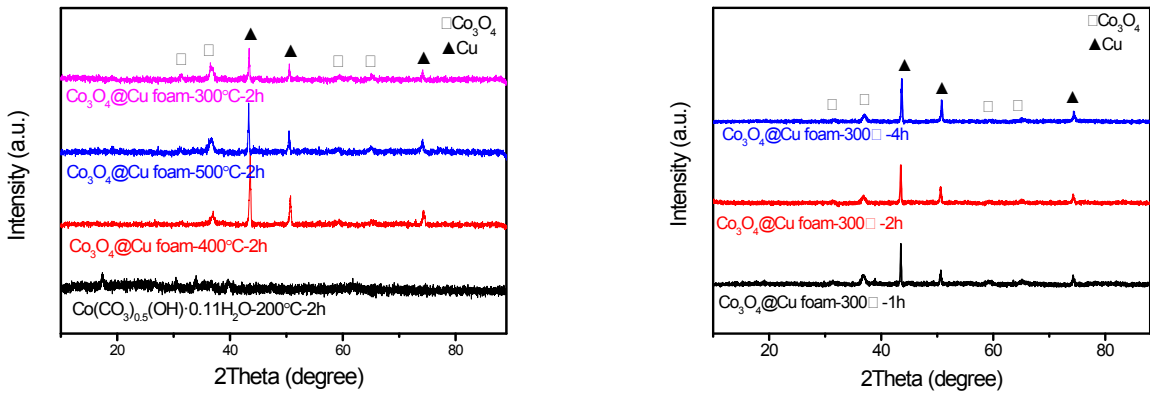


Fig. S2 – XRD patterns of $\text{Co}_3\text{O}_4@\text{Cu}$ foam annealed at different temperatures.

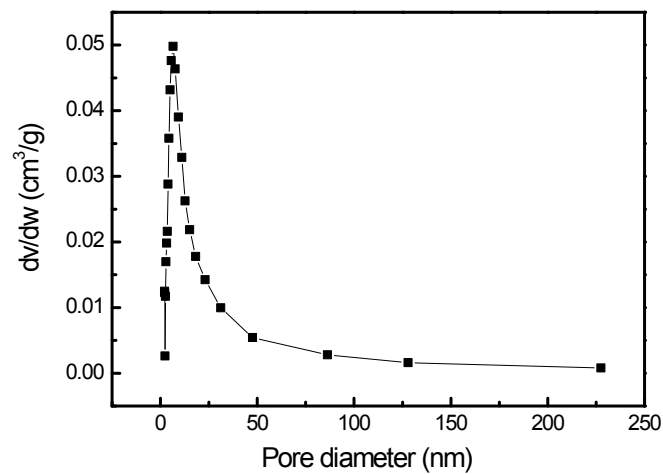


Fig. S3 – BJH pore size distribution of $\text{Co}_3\text{O}_4@\text{Cu}$ foam annealed at 300 °C for 2 h.

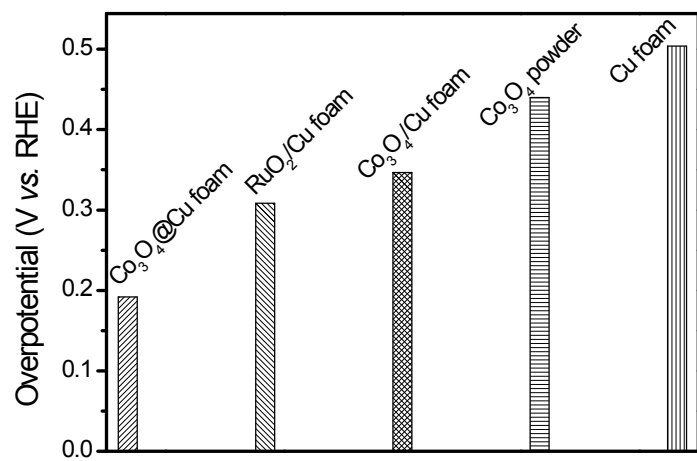


Fig. S4 – Overpotential of Co₃O₄@Cu foam, RuO₂/Cu foam, Co₃O₄/Cu foam, Co₃O₄ powder and Cu foam at 10 mA cm⁻².

Table S1 – The OER performances of our $\text{Co}_3\text{O}_4@\text{Cu}$ foam and previously reported, various Co_3O_4 -based nanocomposites.

Electrocatalyst	Overpotential (mV)	Tafel slope	Testing environment	Reference
	at 10 mA cm ⁻²	(mV dec ⁻¹)		
$\text{Co}_3\text{O}_4@\text{Cu}$ foam	192	42.8	1.0 M KOH	this work
ZnCo_2O_4	390	46	1.0 M KOH	1
$\text{Co}_3\text{O}_4/\text{rGO}$	346	47	1.0 M KOH	2
$\text{G-Co}_3\text{O}_4$	313	56	1.0 M KOH	3
$\text{Co}_3\text{O}_4\text{C-NA}$	290	70	1.0 M KOH	4
$\text{Co}_3\text{O}_4@\text{C-MWCNTs}$	320	62	1.0 M KOH	5
N-doped Co_3O_4 nanosheets	310	59	1.0 M KOH	6
FeCo-ONS	308	36.8	1.0 M KOH	7
$\text{Co}_3\text{O}_4@\text{Ni}$ foam	230	65	1.0 M KOH	8
$\text{Co}_3\text{O}_4@\text{Ni}_3\text{S}_2/\text{Ni}$ foam	260	121.7	1.0 M KOH	9
$\text{Co}_3\text{O}_4\text{-C-NA/Ni}$ foam	310	90	1.0 M KOH	10
$\text{Co}_3\text{O}_4/\text{CoMoO}_4/\text{Ni}$ foam	244	52	1.0 M KOH	11

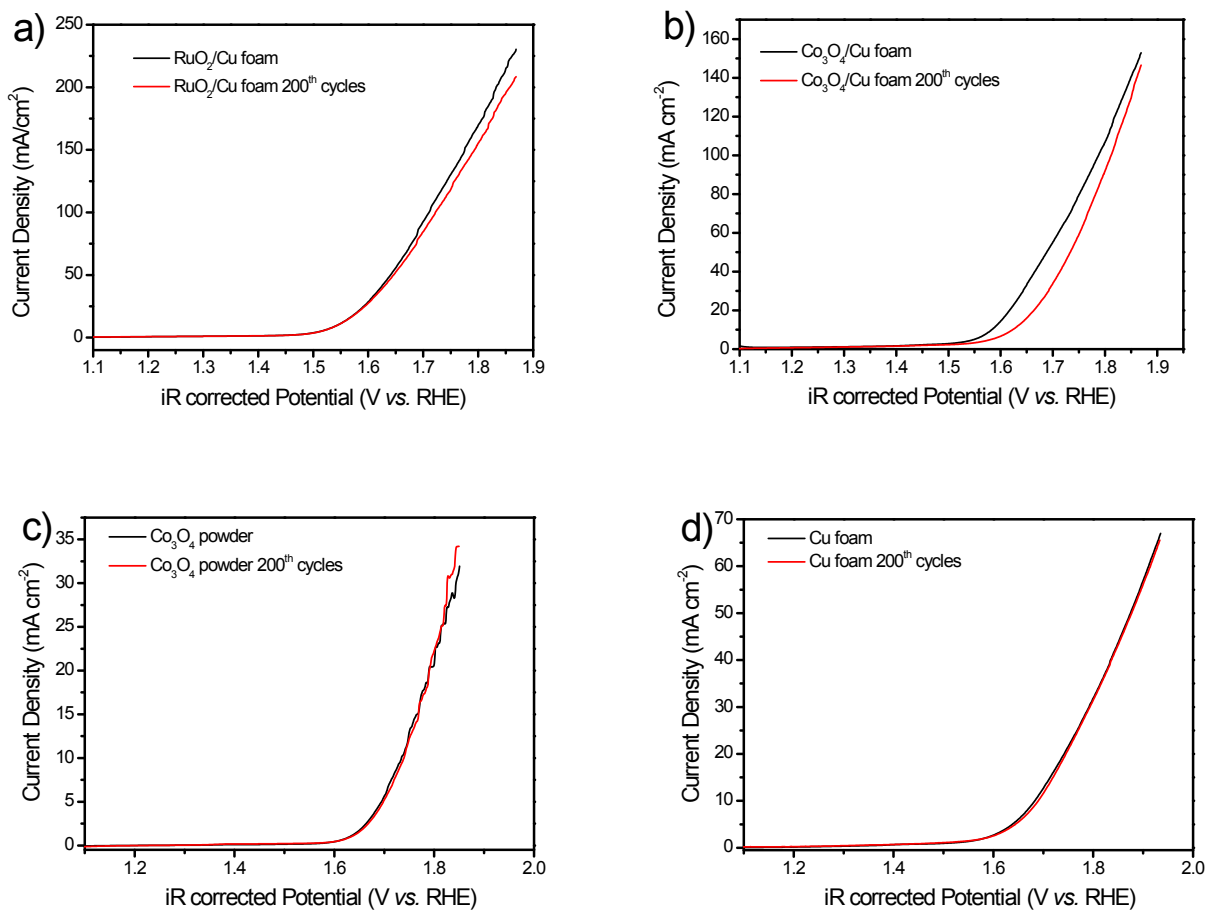


Fig. S5 – LSVs of RuO₂/Cu foam, Co₃O₄/Cu foam, Co₃O₄ powder and Cu foam before and after 200 scans (scan rate = 5.0 mV s⁻¹).

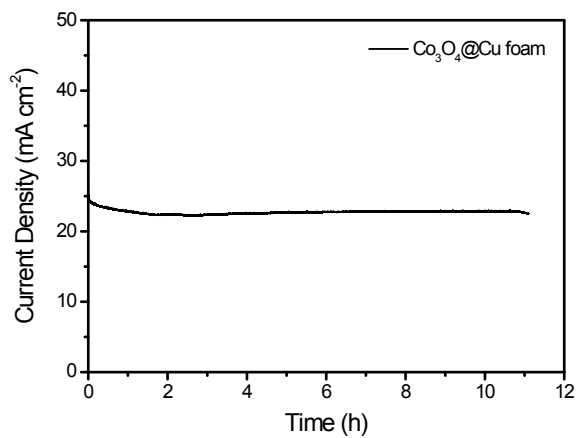


Fig. S6 – Amperometric i-t curve to record long-term durability at the potential of 1.57 V vs. RHE for 11 h.

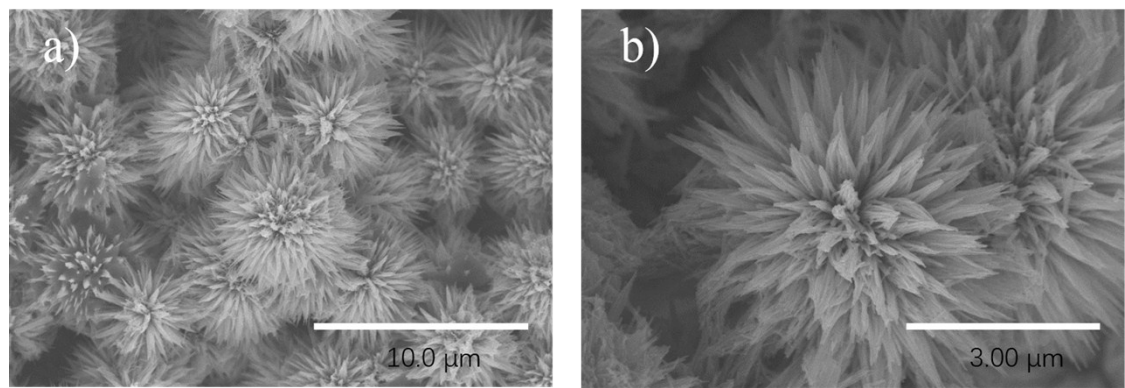


Fig. S7 – (a) Low- and **(b)** high-magnification SEM images of $\text{Co}_3\text{O}_4@\text{Cu}$ foam after OER tests.

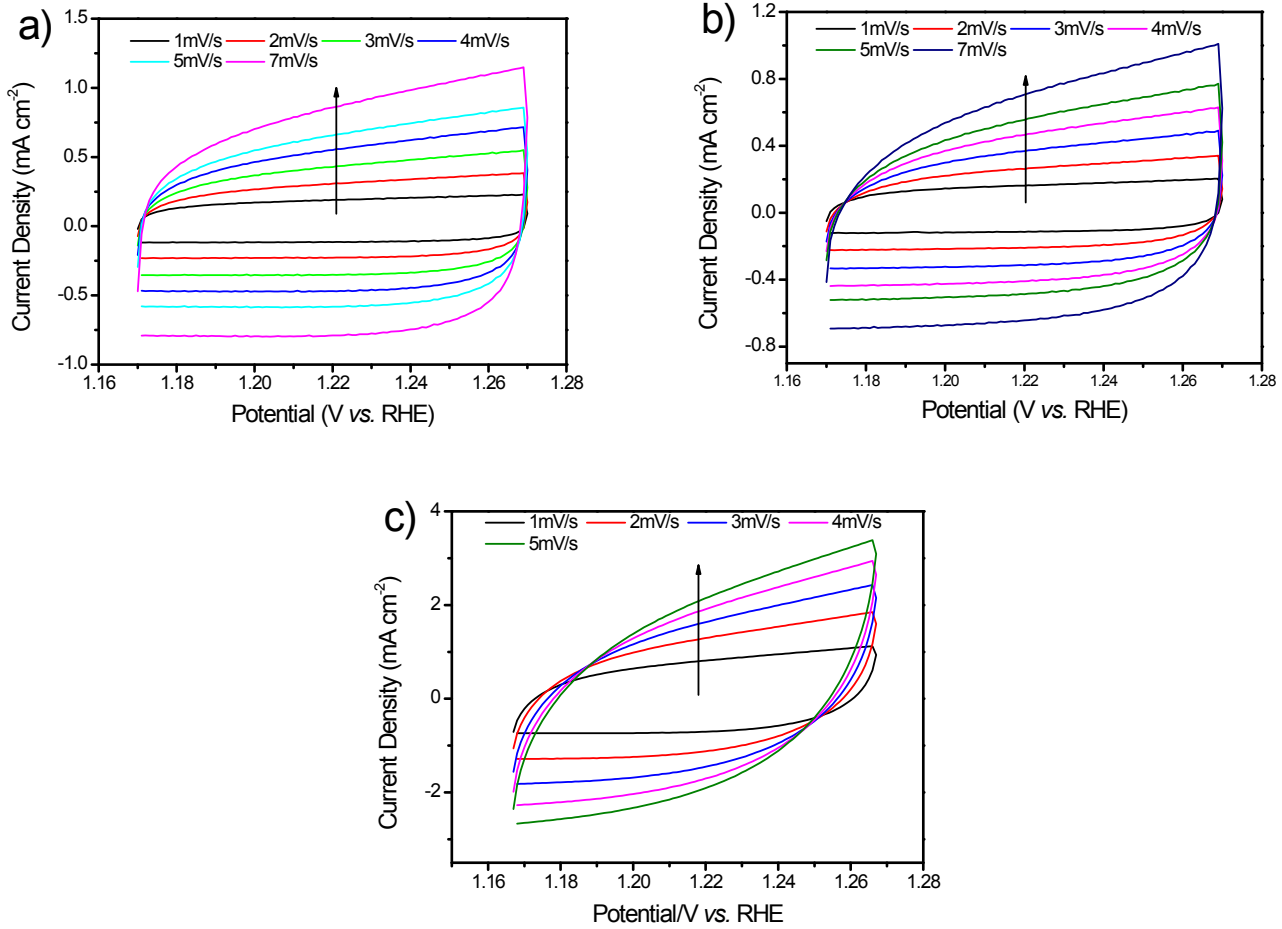


Fig. S8 – EDLC curves of samples with different scan rates. (a) RuO_2/Cu foam, (b) $\text{Co}_3\text{O}_4/\text{Cu}$ foam, and (c) $\text{Co}_3\text{O}_4@\text{Cu}$ foam.

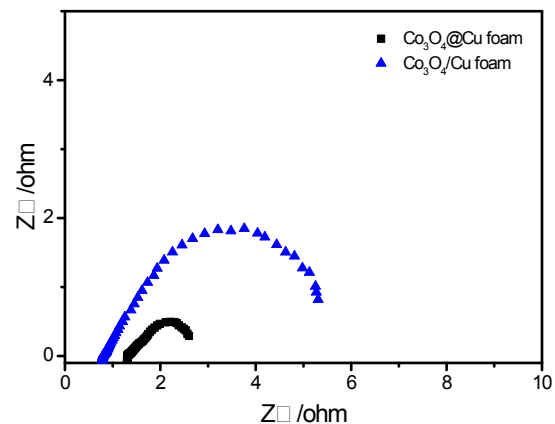


Fig. S9 – Nyquist plots of $\text{Co}_3\text{O}_4@\text{Cu}$ foam and $\text{Co}_3\text{O}_4/\text{Cu}$ foam in 1.0 M KOH.

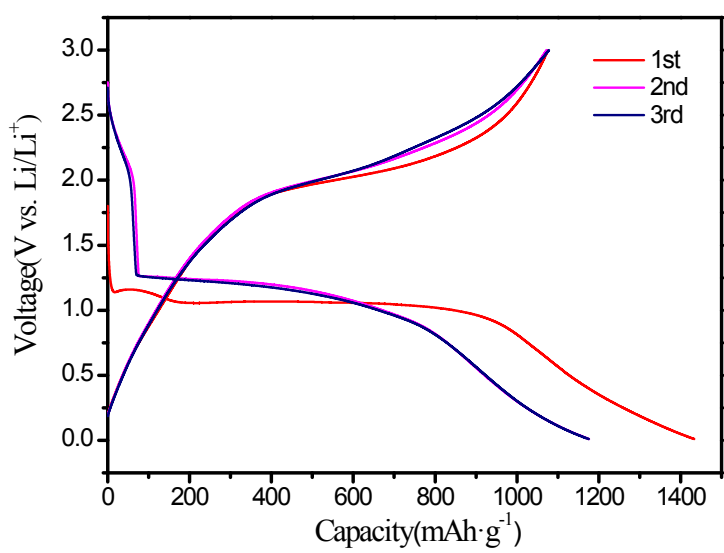


Fig. S10 – Charging–discharging curves of the $\text{Co}_3\text{O}_4@\text{Cu}$ foam electrode at 0.5C.

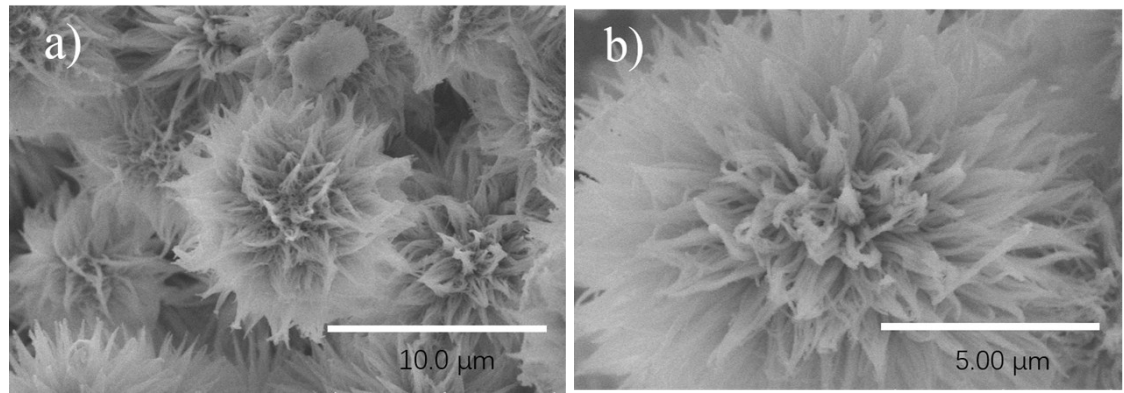


Fig. S11 – (a) Low- and (b) high-magnification SEM images of $\text{Co}_3\text{O}_4@\text{Cu}$ foam after 100 cycles at a current density of 2C.

Table S2 – The cycle and rate performances of our $\text{Co}_3\text{O}_4@\text{Cu}$ foam and previously reported, other Co_3O_4 -based composite anodes.

Samples	Specific capacity (mA h g^{-1}) (cycling numbers) (current density)	High rate capacity (mA h g^{-1})	Reference
$\text{Co}_3\text{O}_4@\text{Cu}$ foam	882 (100) (2C)	626 (5C)	this work
$\text{Co}_3\text{O}_4/\text{C}$	490.5 (50) (0.5C)	676 (2C)	12
Co_3O_4 nanosheets/graphene	851.5 (2000) (2.25C)	509.3 (5.62C)	13
C-doped Co_3O_4 HNFs	1121 (100) (0.22C)	607 (3.4C)	14
N, P-codoped C/ Co_3O_4	927 (100) (0.11C)	454 (1.1C)	15
MWCNTs/ Co_3O_4	813 (100) (0.11C)	514 (1.1C)	16
$\text{Co}_3\text{O}_4/\text{N-PC}$	1730 (100) (0.11C)	560 (11C)	17
$\text{Co}_9\text{S}_8/\text{C-T}$	709 (150) (0.22C)	362 (5.6C)	18
$\text{Co}_3\text{O}_4@\text{CNT}$	862 (60) (0.11C)	408 (5.6C)	19

Supporting References

- 1 T. W. Kim, M. A. Woo, M. Regis and K. S. Choi, *J. Phys. Chem. Lett.*, 2014, **5**, 2370.
- 2 M. Leng, X. L. Huang, W. Xiao, J. Ding, B. H. Liu, Y. H. Du and J. M. Xue, *Nano Energy*, 2017, **33**, 445.
- 3 Y. F. Zhao, S. Q. Chen, B. Sun, D. W. Su, X. D. Huang, H. Liu, Y. M. Yan, K. N. Sun and G. X. Wang, *Sci. Rep.*, 2015, **5**, 7629.
- 4 T. Y. Ma, S. Dai, M. Jaroniec and S. Z. Qiao, *J. Am. Chem. Soc.*, 2014, **136**, 13925.
- 5 X. Z. Li, Y. Y. Fang, X. Q. Lin, M. Tian, X. C. An, Y. Fu, R. Li, J. T. Jin and J. Ma, *J. Mater. Chem. A*, 2015, **3**, 17392.
- 6 L. Xu, Z. Wang, J. Wang, Z. Xiao, X. Huang, Z. Liu, S. Wang, *Nanotechnology*, 2017, **28**, 165402.
- 7 L. Z. Zhuang, L. Ge, Y. S. Yang, M. R. Li, Y. Jia, X. D. Yao and Z. H. Zhu, *Adv. Mater.*, 2017, **29**, 1606793.
- 8 R. C. Li, D. Zhou, J. X. Luo, W. M. Xu, J. W. Li, S. S. Li, P. P. Cheng and D. S. Yuan, *J. Power Sources*, 2017, **341**, 250.
- 9 Y. Q. Gong, Z. F. Hu, H. L. Pan, Y. Lin, Z. Yang and X. Q. Du, *J. Mater. Chem. A*, 2018, **6**, 5098.
- 10 J. T. Ren, G. G. Yuan, C. C. Weng and Z. Y. Yuan, *ACS Sustainable Chem. Eng.*, 2018, **6**, 707–718.
- 11 Z. H. Pei, L. Xu and W. Xu, *Appl. Surf. Sci.*, 2018, **433**, 256.
- 12 J. Chen, X. H. Xia, J. P. Tu, Q. Q. Xiong, Y. X. Yu, X. L. Wang and C. D. Gu, *J. Mater. Chem.*, 2012, **22**, 15056.
- 13 Y. H. Dou, J. T. Xu, B. Y. Ruan, Q. N. Liu, Y. D. Pan, Z. Q. Sun and S. X. Dou, *Adv. Energy Mater.*, 2016, **6**, 1501835.
- 14 C. S. Yan, G. Chen, X. Zhou, J. X. Sun and C. D. Lv, *Adv. Funct. Mater.*, 2016, **26**, 1428.
- 15 Z. F. Wang, X. Zhang, Y. Sun, C. P. Wang, H. Zhang, Y. H. Shen and A. J. Xie, *J. Power Sources*, 2018, **740**, 446.

- 16 G. Huang, F. F. Zhang, X. C. Du, Y. L. Qin, D. M. Yin and L. M. Wang, *ACS Nano*, 2015, **2**, 1592.
- 17 Y. Hou, J. Y. Li, Z. H. Wen, S. M. Cui, C. Yuan and J. H. Chen, *Nano Energy*, 2015, **12**, 1.
- 18 M. K. Wang, J. Zhou, S. Cheng, Q. C. Pan, M. H. Yao, Y. Y. Zhu, P. Wu, H. W. Luo, L. F. Yang and M. L. Liu, *Mater. Lett.*, 2018, **217**, 163.
- 19 D. Gu, W. Li, F. Wang, H. Bongard, B. Spliethoff, W. Schmidt, C. Weidenthaler, Y. Y. Xia, D. Y. Zhao and F. Schuth, *Angew. Chem. Int. Ed.*, 2015, **54**, 7060.